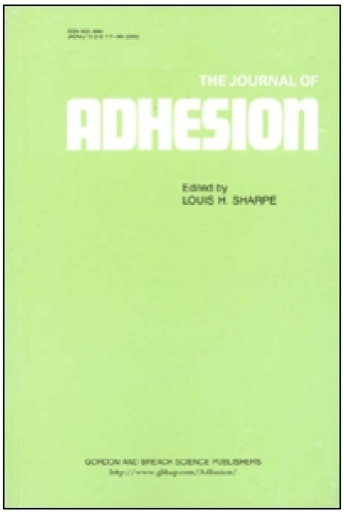

The Journal of Adhesion
Publication details, including instructions for authors and subscription information:
http://www.informaworld.com/smpp/title~content=t713453635

Reactions and Intermediates at the Metal-Polymer Interface as Observed by XPS and NEXAFS Spectroscopy

J. F. Friedrich[a]; I. Koprinarov[a]; R. Giebler[a]; A. Lippitz[a]; W. E. S. Unger[a]
[a] Bundesanstalt für Materialforschung und -prüfung, Berlin, Germany

To cite this Article Friedrich, J. F. , Koprinarov, I. , Giebler, R. , Lippitz, A. and Unger, W. E. S.(1999) 'Reactions and Intermediates at the Metal-Polymer Interface as Observed by XPS and NEXAFS Spectroscopy', The Journal of Adhesion, 71: 2, 297 — 321

To link to this Article: DOI: 10.1080/00218469908014853
URL: http://dx.doi.org/10.1080/00218469908014853

J. Adhesion, 1999, Vol. 71, pp. 297–321
Reprints available directly from the publisher
Photocopying permitted by license only

Reactions and Intermediates at the Metal-Polymer Interface as Observed by XPS and NEXAFS Spectroscopy*

J. F. FRIEDRICH[†], I. KOPRINAROV, R. GIEBLER, A. LIPPITZ
and W. E. S. UNGER

Bundesanstalt für Materialforschung und -prüfung,
Unter den Eichen 87, D-12200 Berlin, Germany

(Received 19 January 1999; In final form 3 May 1999)

Potassium or chromium were evaporated by means of a Knudsen effusion cell under ultra-high vacuum conditions onto a number of common polymers, prepared as stretched foils and spin-coated films. The metal-polymer interface was studied by X-ray Absorption and X-ray Photoelectron Spectroscopy. Evaporated samples were analyzed without exposure to the atmosphere. Different general types of reactions of the metal atoms with the polymers were observed. With deposited K and Cr a redox process including the transfer of substrate oxygen atoms across the interface was found. The formation of π-electron complexes and covalent metal-carbon bonds were obtained exclusively with chromium. Aromatic rings, carbonyl groups and, to a lesser extent, ether linkages are scissioned by metal-polymer interactions. The fourfold substitution of aromatic rings and the exclusive existence of C—O—C structures within polyphenylene ether (PPE) make this polymer most stable toward reactions with chromium. In contrast, bisphenol-A polycarbonate is susceptible to redox reactions with the carbonate group and to forming Cr complexes with aromatic rings using the chromium 3d orbitals. The result is a succession of complex formation, followed by Cr substitution onto aromatic rings and destruction of rings with the formation of chromium carbides.

Keywords: Interfacial polymer-metal redox reactions; chromium-polymer intermediates; near edge X-ray absorption fine structure spectroscopy (NEXAFS); adhesion; polymer-metal bonds; XPS; polymer-aluminum bonds; polymer-aluminum bonds; polymer-copper bonds

---

*Presented at the 4th European Conference on Adhesion (EURADH'98) and 1st World Congress on Adhesion and Related Phenomena (WCARP-1), Garmisch-Partenkirchen, Germany, September 6–11, 1998.

[†] Corresponding author. e-mail: joerg.friedrich@bam.de

1. INTRODUCTION

Investigations of the interaction of metal atoms with genuine building blocks or functional groups of the polymer are important for understanding metal-polymer adhesion. The scope is often broadened also to plasma-produced functional groups at a polymer surface. At the interfaces of polymer-metal composites different types of physical and chemical interactions may occur. Besides electrostatically-enhanced, mechanically-or chemically-induced adhesion, thermodynamic effects also play an important role. Amongst the thermodynamically-controlled interactions, the equilibration of interfacial free energies of the metal and the polymer component results in improved adhesion [1]. One way to converge these energies is a pretreatment of one or both components of the polymer-metal composite; for example, the introduction of polar groups onto nonpolar polymer surfaces by oxygen-plasma treatment [2]. Apart from other postulated mechanism of adhesion, the idea was introduced that a redox reaction with an efficiency depending on the individual polymer substrate and the redox potential of the metal may occur. A thermodynamic equilibrium at the polymer-metal interface is reached by complete conversion of non-noble metal atoms to stable metal oxides or the reduction of a noble metal oxide to its pure metallic state. The equilibrium is characterised by the complete adjustment of interfacial free energies of the metal and the polymer which promotes the adhesion between both components. As known, the interfacial free energy is correlated to the respective redox potential. Table I suggests that the reactions at metal-polymer interfaces are not only thermodynamically controlled (here: by the redox potential) but also strongly kinetically limited. In most cases, additional activation energy (provided by heating or plasma pretreatment) is necessary to initiate the interfacial reaction. Furthermore, diffusion processes of ionised metals and their complexation with carboxylic groups also play an important role. Therefore, after longer storage, polymer regions "far away" from the interface are also chemically changed by diffusing metal ions. Such long-time reactions are basically degradation processes. They result in the formation of a weak boundary layer which decreases the adhesion between metals and polymers.

Some indications of redox reactions and metal-polymer intermediates were found for composites such as polytetrafluoroethylene

TABLE I Interfacial metal-polymer redox reactions after deposition of each 0.4 nm of metal (* analysis of peeled composite interfaces -*cf.* Refs. [1–5]; Ar = arene)

Composite	*Metal*	*Redox potential*	*Polymer structure*	*Plasma activation*	*Thermal activation*	*Other reactions*	*Unchanged structures*	*Redox react. products*
K/PET	K	−2.92 V	—[OOC—phenylene—COO—CH_2—CH_2]—	No	No		C—O—C ?, rings	Carbon, KF
K/PPE	K	−2.92 V	—[(CH_3—)$_2$ arylene —O]—	No	No		C—O—C ?, rings	Carbon, KF
Na/PTFE	Na	−2.71 V	—[CF_2—CF_2]—	No	No			Carbon, NaF
Na/PTFE	Na	−2.71 V	—[CF_2—CF_2]—	Yes	No			Carbon, NaF
Mg/PP*	Mg	−2.38 V	—[CH(CH_3)—CH_2]—	Yes	No		CH—CH_2	MgO
Al/PET*	Al	−1.66 V	—[OOC—phenylene—COO—CH_2—CH_2]—	Yes	Yes	Al…O=C	C—O—C ?, rings	Al_2O_3
Al/PP*	Al	−1.66 V	—[CH(CH_3)—CH_2]—	Yes	No	Al…O=C	CH—CH_2	Al_2O_3
Cr/PET	Cr	−0.71 V	—[OOC—phenylene—COO—CH_2—CH_2]—	No	No	Ar—Cr—Ar, Ar—Cr	C—O—C?	Cr_2O_3
Cr/PE	Cr	−0.71 V	—[CH_2—CH_2]—	Yes	No	Cr..O=C	CH_2	Cr_2O_3
Cr/PE	Cr	−0.71 V	—[CH_2—CH_2]—	No	No	No	Unchanged	No
Cr/PPE	Cr	−0.71 V	—[(CH_3—)$_2$ arylene—O]—	No	No	No	arylene—O—	(Cr_2O_3)
Cr/PMMA	Cr	−0.71 V	—[(CH_3—)—C—($COOCH_3$)—CH_2]—	No	No	Cr..O=C		Cr_2O_3
Cr/PS	Cr	−0.71 V	[CH(phenyl)—CH_2]—	No	No	Ar—Cr—Ar, Ar—Cr		No
CuO/PPQ*	Cu	+0.35 V	—[(phenyl—)$_2$ quinox—O—]	No	Yes	Cu—C		—NO_2, NO, C

(PTFE)—Na, polyethyleneterephthalate (PET)—Al, polypropylene (PP)—Al, PET—Cr, and polyphenylquinoxaline (PPQ)—Cu/CuO during the last 15 years [3–7] (see Tab. I). Alkali metals or copper oxide are very reactive towards functional groups of the polymer. The higher the electropositivity of the metal, the stronger is the reduction reaction. Or, the higher the electropositivity of the metal in the metal oxide, the stronger is the oxidation of the polymeric composite partner. Additional pretreatments or additional activation energy increase the possibility of starting a redox process. The well-known polyethylene (PE) oxidation at the interface with copper-oxide-covered copper in electric cables or the application of the sodium etch process to polytetrafluoroethylene to improve its adhesion properties are strong, not fortuitous, examples of relevant redox reactions between polymers and metals [8]. A number of polymers or organic films (*cf.* [9]) were also coated with submono, mono and multilayers of metals and investigated for indications of the occurrence of redox reactions. Table I summarises some results.

In addition to products of interfacial redox reactions, some stable complexes and ionic and covalent bonds between functional groups of the polymers and metal atoms were identified. Examples for ionic species are Cu^{+1} and $^{-}OOC—$ [10,11]. Many kinds of metal-carbon or metal-oxygen-carbon σ-bonds have a predominant covalent character with more or less ionic bond percentages. Therefore, their stability towards oxidation and hydrolysis is weak. Such bonds are carbides (Me —C) or alcoholates (Me—O—C). The significance of metal—O—C complexes such as Ag—O—C, Mg—O—C, Al —O—C for the improvement in adhesion was emphasized by a number of authors [12–18]. Metal aromatic ring complexes are well-known from metal-organic chemistry. Examples are π-complexes with polyimide [19] and the bisarene-Cr(0) sandwich complex [20–24]. The formation of π-electron complexes from aromatic rings of polymers and metal atoms are limited to transition metals with a high complexing ability. The larger atom diameter of transition elements allows the complexation of six or even more ligands. Especially, this behavior is known from chromium which possesses voluminous 3*d* orbitals. Bonds to six ligands can be formed. This is known from $Cr(CO)_6$, the prototype for the complexation with carbonyls or carbon monoxide molecules liberated by the decarbonylation of bisphenol-A polycarbonate by the interaction with Cr. However, the complexation with aromatic rings is limited to two aromatic rings known as bis-arene chromium(0) sandwich complexes. These complexes are not very stable and undergo dissociation or rearrangements under loss of aromaticity and formation of carbide-like bonds [25–28]. Aromatic rings are discussed in the literature as possible reaction sites but the reactivity and efficiency of such an interaction is contrarily disputed. Therefore, poly(styrene) and poly(phenylene ether) were additionally chosen to represent samples where an interaction of the chromium atoms exclusively with the aromatic ring system or ether oxygen atoms is possible. The purpose of the present work is to identify the possible reaction pathways by comparison of spectroscopic findings obtained with structurally different polymers. From organic chemistry, or from later investigations of metal-polymer interfaces, it is further known that metals can attack carbonyls at the carbon atom (Bouveault-Blanc-like reaction scheme) as well as at the oxygen atom [29].

In this work, changes in the molecular orientation in the uppermost 3 to 5 nm near-surface layer were inspected by the use of angle-resolved Near Edge X-ray Absorption Fine Structure Spectroscopy (NEXAFS). It is well known that the analysis of the C, N, O and F K-edges of technically-relevant polymers is a powerful tool in surface-chemical analysis of polymers [6]. Moreover, surface-sensitive NEXAFS spectroscopy and XPS (X-ray Photoelectron Spectroscopy) provide complementary results [30–32]. XPS gives information on oxidation, carbon-metal bonding, loss in aromaticity or changes in the oxidation state. By NEXAFS spectroscopy, π-bonded species such as $C{=}C$, $C{=}O$ or aromatic rings can clearly be distinguished from σ-bonded species. This is a rather complicated task for XPS because this information can only be obtained by analysis of rather weak shake-up satellites [33].

The sensitivity of the NEXAFS method to π-bonded carbon species can be utilized to contribute to the understanding of the reaction mechanism and the resulting surface state of a polymer surface after metallization. The question of the involvement of aromatic rings, other π-electron bonds [2,4] or the effects on molecular orientation [3] are also of some interest.

2. EXPERIMENTAL

2.1. Polymeric Substrates

The following polymers were used in the investigations: polystyrene (PS), polytetrafluoroethylene (PTFE), polyethyleneterephthalate (PET), polyphenyleneether (PPE or polydimethylphenyleneoxide), polymethylmethacrylate (PMMA), bisphenol-A polycarbonate (PC) and polyphenylquinoxaline (PPQ). Prior to the metallization, all polymer surfaces had been analyzed by XPS to check them for contamination. The relevant binding energies and sub-peak intensity ratios measured were almost identical to those published in the high-resolution XPS spectral database for organic polymers [33].

2.2. Metal Deposition

Metal evaporation was performed inside a preparation chamber (base pressure: 5×10^{-7} Pa) at working pressures better than 1×10^{-6} Pa. This chamber was separated from the analysis chamber by gate valves in both the XPS and NEXAFS experiments. After metallization, the samples were transferred to the measuring position without air exposure. Metals with a purity of 99.97% or better were sublimed from a Knudsen cell onto the substrate through an aperture. The evaporation rate (ca. 0.1 nm min^{-1}) was determined by a quartz microbalance placed at the sample position. In any case, specimens with individual metal overlayer thickness were prepared starting with a new sample from the same polymer batch.

It is well-known that evaporated metals such as K and Cr getter oxygen from ambient oxygen-containing species at very good vacuum conditions. To avoid misinterpretations, after every evaporation the O/C atomic ratio was checked by XPS to distinguish the oxygen effect with residual gas from the polymer-oxygen interaction.

2.3. X-ray Photoelectron Spectroscopy (XPS)

XP spectra were measured with an oil-free-pumped ESCALAB 200X electron spectrometer (VG Scientific, East Grinstead, UK). Mg Kα excitation (15 kV, 20 mA) was used for spectra acquisition. The analyser was operated at a fixed-retarding ratio of 40. Electrons were accepted at a 20° take-off angle. The operating pressure of the vacuum system during the data acquisition was better than 5×10^{-7} Pa whereas the base pressure of the system is 1×10^{-8} Pa. XPS data processing and quantification were performed using routines which are part of the SCIENTA ESCA 300 (SCIENTA AB, Uppsala, Sweden) and the VGS Eclipse (VG Scientific, UK) data systems. For the estimation of relative intensities (atomic ratios), Scofield's cross sections were used [34]. The error of the quantitative data was assessed to be better than ±20%. The fits of the XPS narrow scans were set-up according to Ref. [33]. The charging of the surface of the thin polymer samples investigated in this work is stabilized by electrons provided by the Al X-ray window of the X-ray gun. All samples were prepared on grounded sample holders with the help of double sided conductive adhesive pads. The charging was corrected by using the most prominent C1s feature using binding energy values taken from Ref. [33].

2.4. X-ray Absorption Spectroscopy

NEXAFS spectroscopy was carried out on the HE-TGM-2-monochromator [35, 36] beam line at the synchrotron light source BESSY (Berlin, Germany) [37]. The resolution of this monochromator was estimated to be 0.8 eV at the C K-edge. Detailed data are given elsewhere [6]. The calibration of the energy scale of the monochromator was performed using the first and second-order chromium-L-edge contributions measured with a thick Cr metal deposit. Subsequently, the energy scale of the monochromator was adjusted using the graphite $C1s \rightarrow \pi^*$ resonance energy, measured with a pyrolitic graphite sample (Advanced Ceramic Corp., Cleveland, Ohio). This resonance was set to 285.4 eV [38].

Absorption was measured by monitoring photoelectrons as well as C-KLL, O-KLL, and Cr-L series Auger electrons [6]. The measurements were carried out in the partial electron yield (PEY) mode where low-energy electrons are suppressed by a preset threshold energy of 150 eV. The resulting information depth [39], defined to be the depth from which 95% of the detected electrons originate, was estimated to be ≈ 3.0 nm for the C K-edge and ≈ 5.0 nm for the O K-edge as well as the Cr L-edge signals [40]. Here it was assumed that the above-mentioned Auger electrons dominate the signal measured in the experiment.

Most of the NEXAFS spectra were recorded at an angle of 55° between the surface normal of the sample and the electric field vector, ***E***, of the incident radiation. At this angle, the signal intensity does not depend on the molecular orientations of the sample [4, 5] .The X-ray-spot area was $\leq 1\,\mathrm{mm}^2$. During the data acquisition, the operating pressure of the vacuum system was better than 1×10^{-7} Pa (base pressure of the system is 2×10^{-8} Pa). The reproducibility of the spectra was checked by multiple scanning. Beam damage effects were not found.

Unfortunately, the chromium L-edge superimposes on the second order of the C K-edge spectrum. Therefore, this second order contribution was quantitatively measured with a pure Cr sample to be 6% of the first-order Cr-$L_{2,3}$-edge signal intensity for the HE-TGM-2 monochromator configuration used for the experiments. Accordingly, the NEXAFS spectra measured after the metallization are, when needed, corrected for the Cr L-edge second-order contributions.

3. RESULTS

3.1. Redox Reaction Between K, Na, Al, Cr or Cu with O or F Functional Groups of a Polymer

3.1.1. Potassium/sodium

Evaporation of K or Na mono-or multilayers of atoms onto graphite-filled PTFE have caused dramatic changes in elemental composition. In the XP spectra of a PTFE film, a strong shift in the C1s binding energy from 292 eV to ca. 283 eV were detected after K multilayer evaporation. These results together with a blackening of the PTFE surface are taken as a proof for the existence of elemental carbon at the surface (Fig. 1).

K was evaporated with different layer thickness on PET and was analysed by NEXAFS spectroscopy. The C and O K-edge spectra of PET films were measured (Fig. 2). Table II compares the decrease of selected resonance intensities after each 0.4 nm deposition of K. It can be concluded from Table II that K reacts as a strong reducing agent (redox potential $E^\circ = -2.92$ V, *cf.* Tab. I) because it preferentially attacks oxygen in PET, especially the $>\mathrm{C{=}O}$ group, as seen in the O K-edge spectrum (*cf.* Fig. 2).

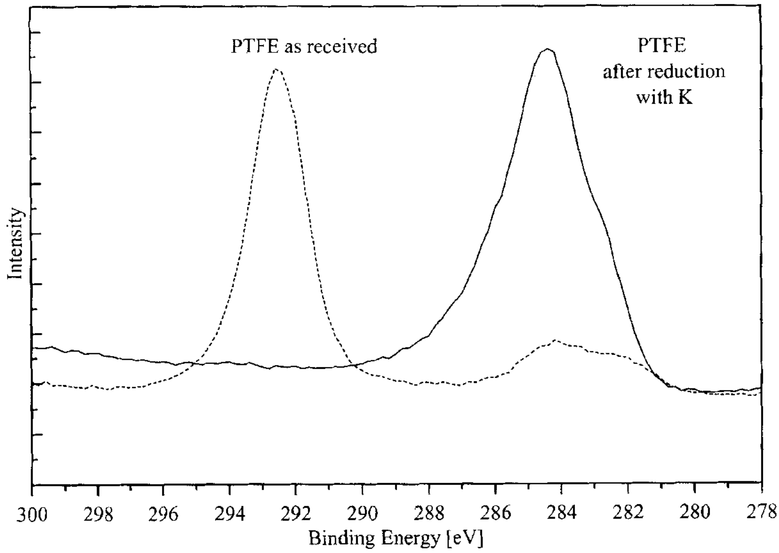

FIGURE 1 C1s XP spectra of PTFE (with 5% graphite filler) before and after deposition of ≈ 10 nm of potassium and subsequent rinsing in distilled water.

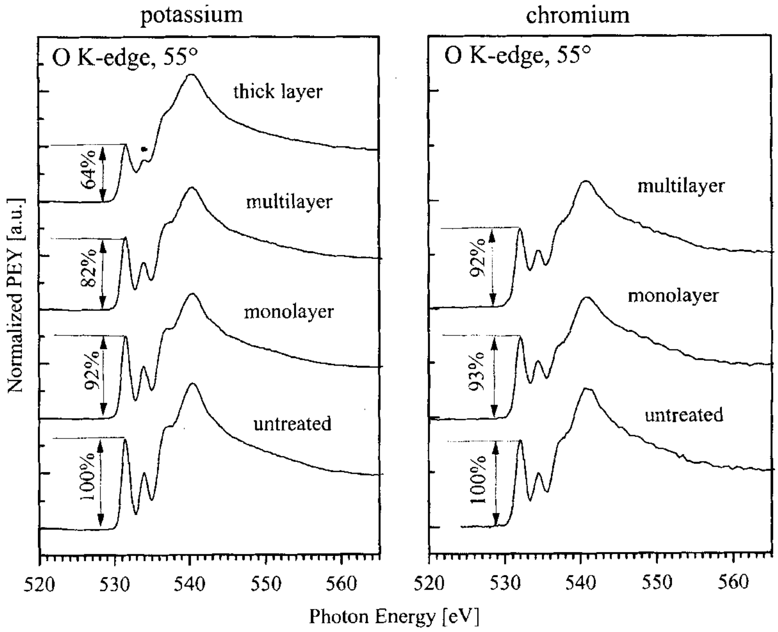

FIGURE 2 NEXAFS O K-edge spectra of PET before and after deposition of potassium and chromium (nominal metal film thickness: ≈ 0.15; ≈ 0.4; ≈ 2.00 nm).

TABLE II Changes in selected PET NEXAFS C and O K-edge resonance intensities after deposition of nominally 0.4 nm K and Cr

Transitions	$C1s \rightarrow \pi^*_{ring}$	$C1s \rightarrow \pi^*_{C=O}$	$O1s \rightarrow \pi^*_{C=O}$
K	Nearly unchanged	− 36%	− 36%
Cr	−35%	− 10%	− 8%

3.1.2. Aluminium

Al is also a strong reducing agent ($E^\circ = -1.66\,\text{V}$) towards oxygen-or fluorine-containing polymers. This could be demonstrated with CF_4 plasma modified PET which was evaporated with an Al film. The $C{-}F_n(n = 1-3)$ bonds formed at the PET surface react with Al resulting in the formation of AlF_3. This was evidenced by the analysis of the XPS Fls peak (BE = 76.5 eV) taken from the inner side of the peeled-off Al overlayer. The same phenomenon was also observed when PET surfaces were fluorinated in the gas phase in 95% $Ar/5\%F_2$ [41]. Oxygen-containing groups at PET surfaces, produced by an oxygen plasma modification, react with Al to Al_2O_3 and, most probably, to $Al...O{=}C<$ complexes. These results indicate a redox reaction between Al and carbonyl sites within the ester group of PET [16, 42]. However, the high affinity of Al to oxygen does not only result in reactions with oxygen bound in the macromolecules but also with oxygen from adsorption layers on the walls of the evaporation chamber, from residual gas, or leakage flow. Therefore, the experiments with fluorinated PET surfaces show the predominance of the reaction at the interface. Here, the redox reaction occurs with fluorine instead with oxygen and, therefore, this reaction cannot be superimposed by traces of oxygen from sources far from the interface.

3.1.3. Chromium

Cr is less reactive towards carbonyl groups than K (*cf.* Tab. I and Fig. 2). This results from the lower redox potential for the Cr° to Cr^{3+} transition ($E^\circ = -0.71\,\text{V}$). However, it could be clearly demonstrated by an evaluation of XPS O1s spectra and NEXAFS O K-edge spectra that carbonyl groups are reacting with Cr deposits (see also Refs. [12–18]). Carbonyl structures in PET (Fig. 2), PMMA and bisphenol-A polycarbonate (Fig. 3) differ in their sensitivity towards Cr attachment and subsequent degradation.

A nominally 0.4 nm thick Cr layer diminishes the C=O content at the PET or PMMA surface by 8% but at the PC surface by 77%. It is obvious that the carbonyls in the ester groups of PMMA and PET are much more stable than the C=O unit in the carbonate group of PC. In the XP O1s spectra of PC (Fig. 4) and of PET (not shown), and PMMA (not shown), new sub-peaks at BE = 530.5, 529.7 and 531.3 eV, respectively, were obtained. The low binding energy feature is interpreted to result from the formation of Cr oxide species (Cr_2O_3) comprising about 20, 10 or 27% of the total oxygen in the analyzed surface layer.

PPE includes exclusively ether linkages of the phenylene rings. These were also attacked by chromium. By considering the XPS O1s subpeak at BE ≈ 531 eV, nearly 35% of the total O surface atoms can be assigned to chromium(III) oxide (Fig. 5).

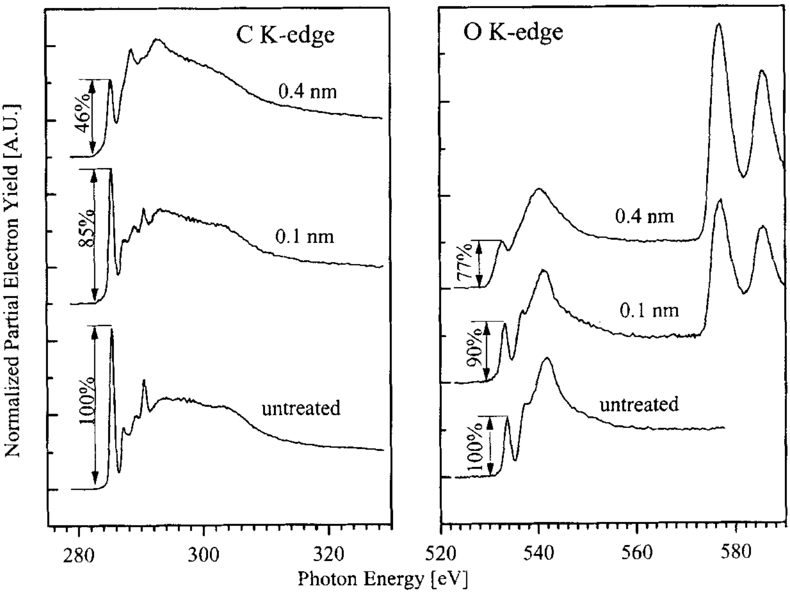

FIGURE 3 NEXAFS O and C K-edge spectra of bisphenol-A polycarbonate before and after deposition of chromium (0.1 and 0.4 nm).

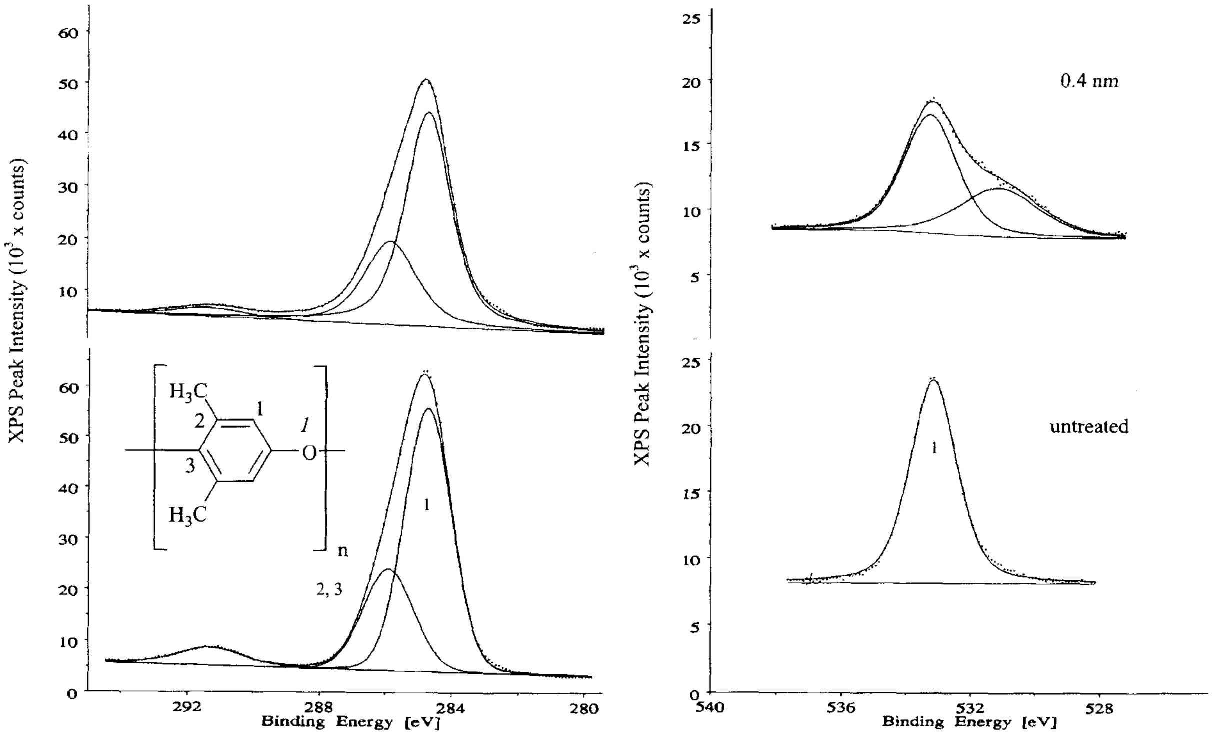

FIGURE 4 C1s and O1s XP spectra of PPE before and after deposition of ≈0.4 nm of chromium.

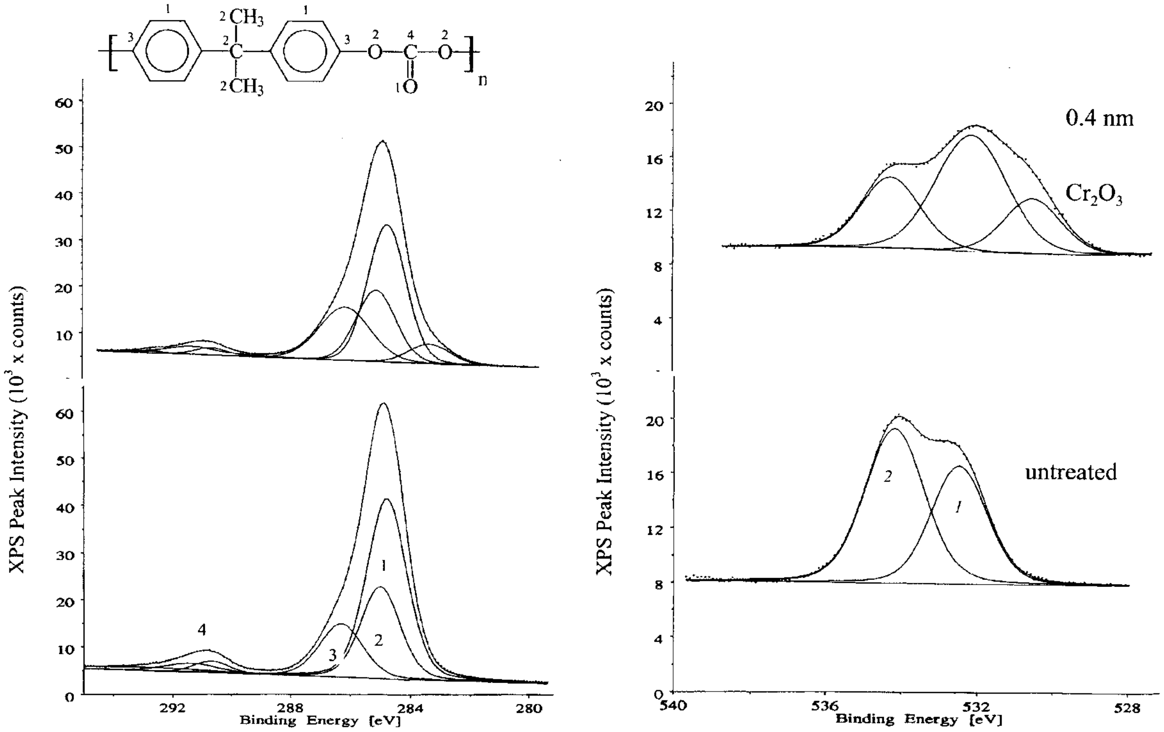

FIGURE 5 C1s and O1s XP spectra of PC before and after deposition of ≈0.4 nm of chromium.

The consumption of oxygen from carbonyl groups and, to a lesser extent, ether linkages, to form Cr(III) oxide can be understood in terms of a redox process.

3.1.4. Copper

A positive redox potential of the metal component as existing in copper-polymer composites ($E^\circ = +0.41\,\mathrm{V}$) gives rise to an oxidation of the polymer component. For instance, this was exemplified by the Cu/CuO/PPQ composite in the mid-1980s [1]. Thin CuO layers on metallic Cu interact with aromatic quinoxaline and phenyl rings of PPQ to form N=O, NO_2 or NO_3 groups. Ring destruction and formation of gaseous oxidation (degradation) products such as NO or NO_2 also occurred. Simultaneously, a reduction of CuO to Cu was observed supporting the idea of a redox reaction [1, 43]. Here, a list (Tab. III) can be presented showing the partial reduction of copper(II) oxide by PPQ.

After peeling a PPQ film from an oxidized copper substrate a very thin layer of oxidized PPQ remains at the copper substrate as seen in the XP spectrum by remaining C and N signals. Their intensity ratio was found to be characteristic for PPQ. The reduction of CuO is evident by the decrease of the $Cu2p_{3/2}$ satellite from 47 to 27 referenced to the intensity ratio between the $Cu2p_{3/2}$ peak and $Cu2p_{3/2}$ satellite of 100:55 for pure CuO (*cf.* Tab. III) [44].

3.2. Reaction Between Aromatic Rings in Polymers and Metals

Some stable and metastable, chemically-bonded, metal-polymer intermediates are formed at the interface independently of the redox

TABLE III Relative XPS intensities (elemental ratios) at the copper (copper oxide) and PPQ interfaces of a peeled copper (copper oxide)-PPQ polymer composite (* satellite between the $Cu2p_{3/2}$ and $Cu2p_{1/2}$ XPS peaks)

Material	*C1s*	*O1s*	*N1s*	*Cu2p$_{3/2}$*	*Satellite**
PPQ stoichometric	100	7	14	–	–
PPQ as synthesized [1]	100	10	12	0	0
CuO stoichometric [30]	–	100	–	100	55
oxidized copper surface	13	87	0	100	47
PPQ interface	100	12	10	0	0
copper interface	75	94	7	100	27

reactions. One intermediate is the complexation of transition metals with aromatic rings in polymers. The mechanism of the interaction of chromium with PET is an example. The Cr attack toward ester carbonyl groups is another reaction pathway as mentioned before. The extended 3d orbitals of Cr interact strongly with the aromatic rings as shown by Pireaux's quantum chemical calculations for Cr-PMDA-ODA [45]. This is also true for the PET case as verified by Figure 6.

Here, A and A' are $\mathrm{C1s} \rightarrow \pi^*_{\mathrm{ring}}$ resonances. Compared with the non-metallized state, the ring intensity is decreased by deposited increments of Cr indicating the destruction of aromatic rings by about 35% (*cf.* Tab. II).

K did not react with aromatic rings as verified by the stable $\mathrm{C1s} \rightarrow \pi^*_{\mathrm{ring}}$ resonances. However, reaction with carbonyl groups seems to be effective as revealed by the changes of the $\mathrm{O1s} \rightarrow \pi^*_{\mathrm{C=O}}$ resonance intensities (*cf.* Fig. 2). Other aromatic polymers (PS, PC) also show losses in aromaticity in the range of 54 to 35% as a result of

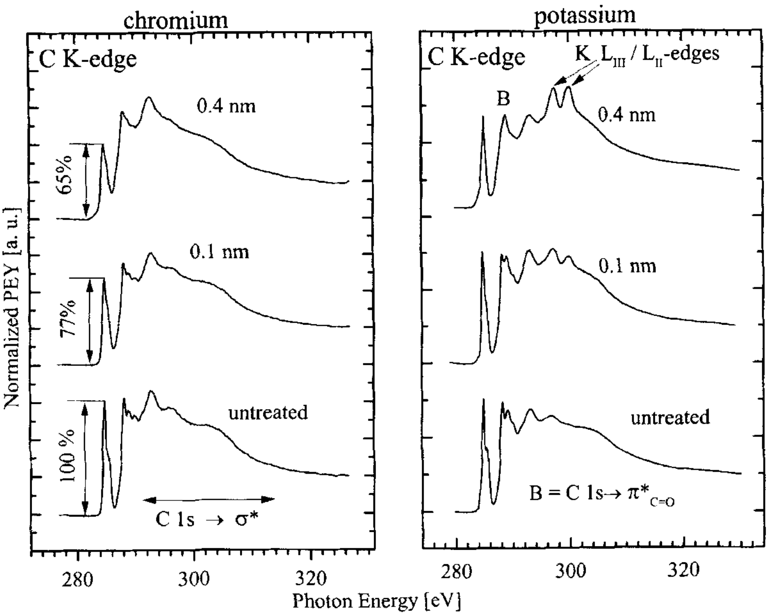

FIGURE 6 NEXAFS C K-edge spectra of PET before and after deposition of potassium and chromium.

deposited Cr (*cf.* Fig. 4). The fourfold substituted aromatic ring in PPE was found to be much more stable in these experiments as indicated by only a 15% decrease in aromaticity after depositing 0.4 nm Cr (*cf.* Fig. 5).

3.3. Special Reaction Behaviors of PS, PET, PC and PPE

Table IV reveals strong differences in the response of PET and PC to the evaporation of ca. 4 monolayers of Cr. Nearly all carbonate groups represented by the C1s → $\pi^*_{C=O}$ resonance and 54% of aromatic rings of the PC are destroyed, as monitored by NEXAFS C K-edge spectra. Ester carbonyl groups in PET are obviously more stable against Cr attack.

Also, strong interactions of Cr with aromatic rings were observed with a PS film assigned by the occurrence of a shoulder at the C1s → π^*_{ring} resonance (Fig. 7). The mobility of phenyl rings promotes the formation of bis-arene Cr sandwich complexes as illustrated by the insert.

Additionally, XPS of Cr-evaporated PS revealed a new subpeak at 283.1 eV. This peak is attributed to Cr—C bonds. The relatively broad C—Cr XPS peak (FWHM ≈ 2 eV) shown in Figure 5 was also observed with Cr-metallized polycarbonate, here at a binding energy of BE ≈ 283.5 eV. Results covering the attack of chromium to aromatic rings of these polymers are summarized in Table V. The 2, 5-CH_3 substitution of the aromatic ring of PPE provides protection toward the formation of Cr—C bonds as confirmed by Table V. This is in good correlation with the low percentage of formed Cr-arene complexes. Therefore, it is likely that the π-metal-arene complex is a precursor of the chromium-carbide formation.

TABLE IV Comparison of the degradation behavior of C=O groups and aromatic rings of PC and PET resulting from the deposition of 0.4 nm Cr as deduced from the respective decreases in the intensity of O1s → $\pi^*_{C=O}$, C1s → $\pi^*_{C=O}$ and C1s → π^*_{ring} resonances

Polymer	*C=O + Cr* (*C1s* → $\pi^*_{C=O}$)	*C=O + Cr* (*O1s* → $\pi^*_{C=O}$)	*Arene + Cr* (*C1s* → π^*_{ring})
PET	90%	92%	65%
PC	22%	77%	46%

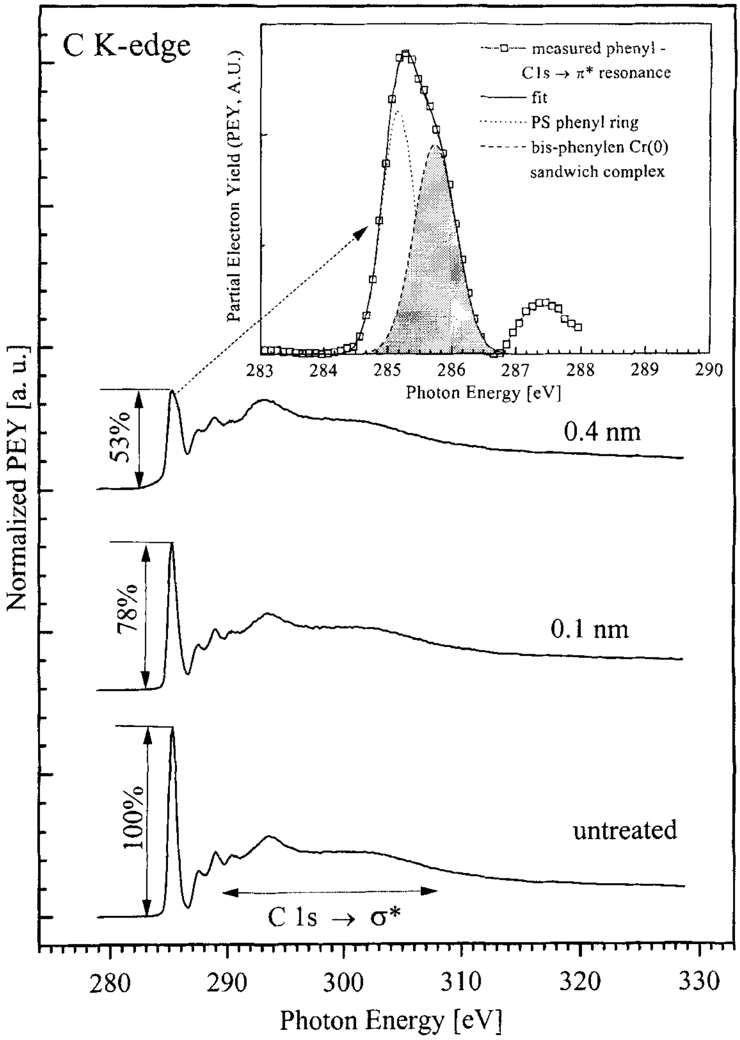

FIGURE 7 NEXAFS C K-edge spectra of PS before and after deposition of chromium with a zoomed C1s → π^*_{ring} resonance region as an insert. The peak of the bisphenyl-Cr(0) sandwich complex is presented in grey.

TABLE V Relative height [%] of the C1s → π^*_{ring} resonance in the C K-edge spectra of different polymers after deposition of 0.1 or 0.4 nm of Cr

Cr thickness	*PPE*	*PC*	*PET*	*PS*
0.1 nm	95	85	77	78
0.4 nm	85	46	65	53

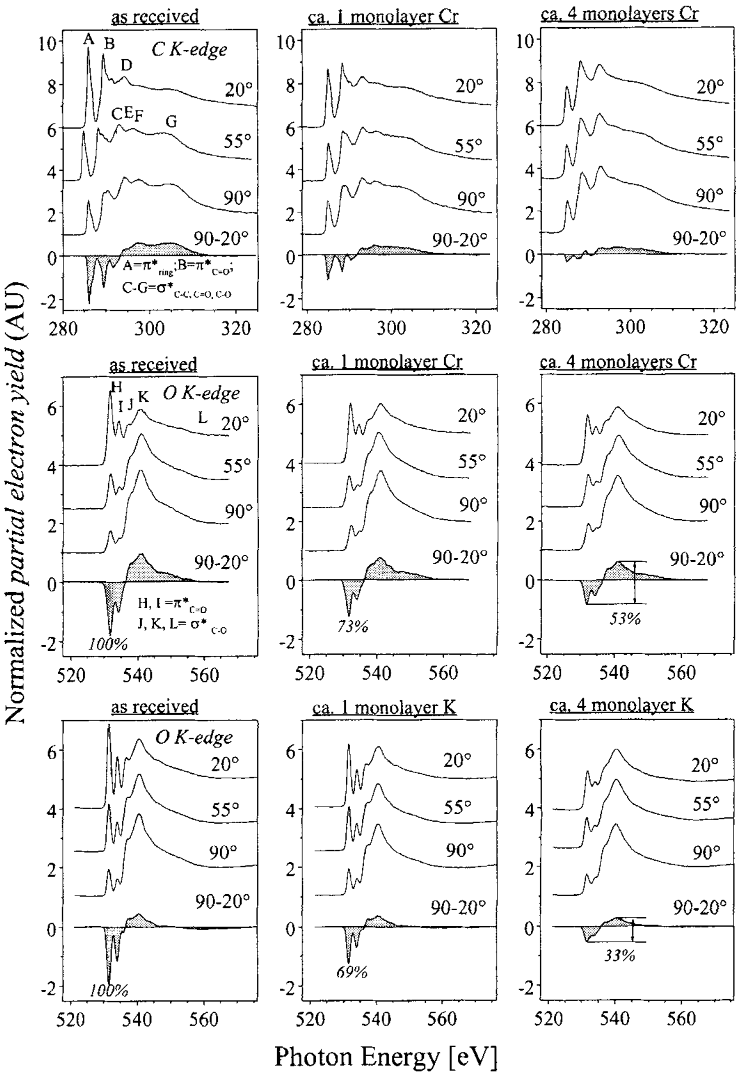

FIGURE 8 Set of angle-resolved C and O K-edge spectra of PET for different thicknesses of chromium and potassium. The information depth of the C K-edge is about 3 nm and that of the O K-edge about 5 nm. The italic percentages at the O K-edge difference spectra represent the decrease in the amplitude of PET values roughly referencing the loss in anisotropy.

3.4. Cr-Polymer Intermediates and Reactions

Four principal types of reaction products may be deduced from the spectroscopic results:

(1) a Cr—aromatic ring complex intermediate,
(2) two Cr—C carbide-like species (Cr_2—C_2 cyclic and Cr—C) from the attachment of two Cr to the aromatic ring or to cracked ring fragments or other fragments (PMMA),
(3) products of reactions with the carbonyl group, such as Cr—C—OH, Cr—O—C, and
(4) the formation of Cr_2O_3 characteristic for a redox reaction.

3.5. Disorientation Effects of Macromolecular Structures by Evaporated Cr and K Monolayers

The anisotropic supermolecular structure of biaxially-stretched PET foils is destroyed by Cr evaporation in a very thin surface layer. This was concluded from the observation of linear dichroism phenomena in angle-resolved NEXAFS spectroscopy experiments on multilayer deposits of chromium and potassium on PET (Fig. 8).

The 90-20°C K-edge difference spectrum verifies a complete loss of anisotropy, whereas in the O K-edge case the elongation in the respective difference spectrum is slightly decreased for chromium and stronger for potassium (*cf.* Fig. 8). Considering the different information depth of the C and O K-edges, a thickness of around 2 nm can be deduced for the disoriented surface layer of the PET sample. The Cr-PET and K-PET interaction layers are characterized by a disorientation of the complete supermolecular structure to an isotropic state.

4. DISCUSSION

Two principal types of reactions between polymers and metals at the interface were identified:

(a) permanent and metastable metal-polymer bonds and interactions, as well as
(b) redox reactions with oxygen or fluorine species exchanged across the interface which are accompanied by an adjustment of the interfacial free energies of both composite partners.

Covalent bonds between the components at a metal-polymer interface should result in strong and durable adhesion. However, metal-carbon or metal-oxygen-carbon bonds are not purely covalent bonds. They contain more or less high ionic contributions, predicting a susceptibility to bond weakening by, for example, hydrolysis. Complexation of metal atoms with π-electron-containing bonds or ring systems often result in weak and unstable bonds, characterized by a tendency to rearrange.

It is known from simple metal organic chemistry that π-electron complexes of transition metals and functional groups of polymers often decompose or rearrange. Chromium forms slightly stable π-electron complexes with aromatic rings as well as with carbonyl groups as shown in Figure 9.

This could be confirmed by comparison with the respective NEXAFS spectra of some arene—Cr, CO—Cr and arene—CO—Cr model complex substances [46]. The most favored complex is the bisarene chromium(0) sandwich complex as detected with atactic polystyrene. The phenyl side groups can easily undergo steric disorientations to form such a sandwich at relatively low activation energies. In polyethyleneterephthalate and bisphenol-A polycarbonate, the aromatic phenylene rings are fixed in the polymer backbone. Additionally, the supermolecular structure produced by stretching or freezing of films results in such a thermodynamically-unstable orientation. In this case, mono-arene complexes with chromium or a very unstable distorted bis-arene Cr complex are more plausible. With polycarbonate, the easy loss of the carbonate groups from interactions with chromium (*cf.* Fig. 9) suggests the participation of free carbon monoxide to form mixed complexes consisting of arene and $C\equiv O$.

Moreover, the attachment of chromium to the aromatic rings by chemical bonds was observed to initialize the formation of metastable Cr—C species which are bound in a four-membered ring (—Cr—Cr—C—C—) and attached to the aromatic ring (*cf.* Fig. 9) similar to the reaction of Mo(110) with benzene or benzenethiol (*cf.* [47, 48]). This was definitively indicated from XP spectroscopy by a low-binding-energy C1s subpeak at $E \approx 283.8\,\text{eV}$. A second low-binding-energy C—Cr species is probable ($\text{BE} \approx 283.0\,\text{eV}$) which should represent a non-stoichiometric chromium carbide from a decomposed aromatic ring [6]. The species was also mentioned in the

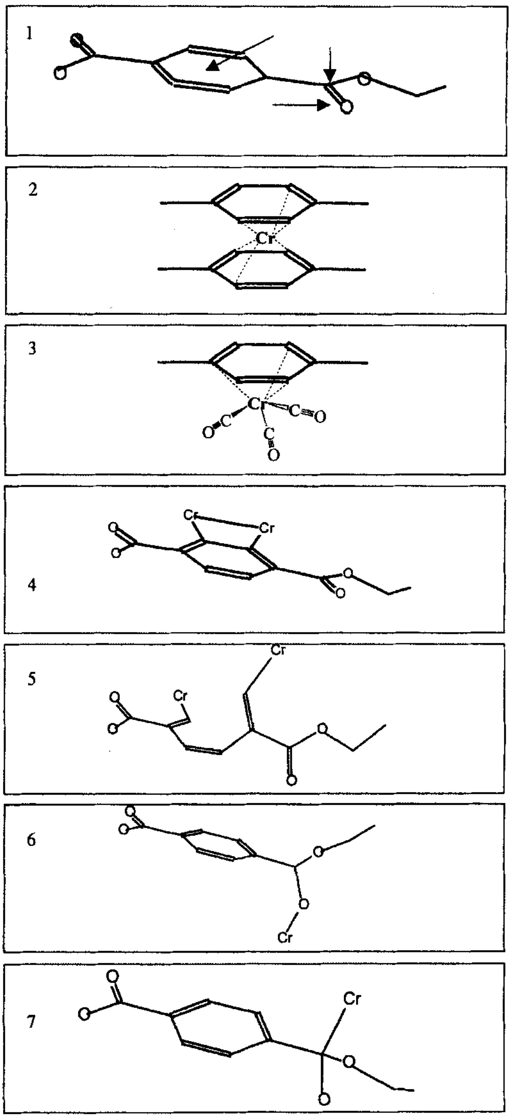

FIGRUE 9 Calculated (MM2) models of Cr-polymer (H-terminated cut of a PET macromolecule) intermediates: (1) attack of Cr onto PET (marked with arrows); (2) formation of a bisarene-Cr(0) sandwich complex; (3) monoarenetricar-bonyl-Cr(0) complex; (4) Cr-ring bicycle; (5) chromcarbide; (6) torsion of the ester group by 90° caused by C—O—Cr interactions; (7) Cr—C—OH formation (analog of Bouveault-Blanc reaction).

literature cited before [47, 48]. We assume the successive decomposition of the bis-arene Cr(0) sandwich complex by addition of a further Cr atom to the

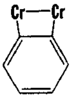

ring and, subsequently, to the non-stoichiometric Cr—C species.

Chromium also reacts with carbonyl groups forming π-electron complexes with $Cr^{\delta+} \ldots O^{\delta-} \doteq C^{\delta+}$ that are often described for all metals interacting with carbonyls ($Me^{\delta+} \ldots O^{\delta-} \doteq C^{\delta+}$, *cf.* Ref. [12]). From the chemist's point of view, an attack on the "positive-partially" charged carbonyl C atom is also possible as described in the scheme given in Figure 9. C—OH groups are formed then. This reaction scheme is known as the Bouveault-Blanc reaction. The final redox reaction (1) can be formulated as:

$$\text{Polymer}(C = O, C—O) + 2Cr \rightarrow \text{polymer} + Cr_2O_3 \qquad (1)$$

The reaction of potassium with carbonyl groups of C—O species is evidence for the occurrence of a redox reaction. As reported elsewhere, it could be shown that oxygen-functionalized octadecyl trichlorosilane self-assembled layers also undergo a redox reaction with Cr [49–51]. Here, Cr reacts, similarly to K, with C = O and also with the C—O—species of the polymer structure. This could be demonstrated with PET, PC, PMMA and, to a much lower extent, with PPE. In contrast to these carbonyl-group-containing polymers, PPE has only ether bonds. However, the analysis of the XPS Ols peak has shown that the formation of a considerable percentage of Cr_2O_3 indicates also the destruction of C—O—C bonds, thus providing a redox reaction scheme.

5. SUMMARY

A shoulder at the high energy side of the π^*_{ring} resonances was interpreted to be a finger print of a Cr-arene complex existing at the surface. $(CO)_3(arene)Cr^0$ may also exist. A low-energy subpeak in the Cls XP spectra was observed and interpreted as Cr-substituted aromatic rings or Cr carbide. Cr or K deposition on oxygen-containing polymers results in a redox reaction in which Cr(III) or K oxide are formed. A mechanism is proposed for the Cr attack on C=O groups beginning with an intermediate charge transfer complex and ending with a carbonyl site reduced to C—OH. Disorientation of functional groups and also of near-surface segments of polymers may result from deposited Cr.

Acknowledgements

We thank Ch. Wöll and K. Weiss from the Ruhr University in Bochum as well as Dr. K. Braun from BESSY mbH, Berlin, for collaboration during the NEXAFS experiments. The *Deutsche Forschungsgemeinschaft* (*DFG*) has sponsored this project under grant number Fr 975/1-3.

References

[1] Friedrich, J. F., Falk, B., Loeschcke, I., Rutsch, B., Richter, Kh., Reiner, H.-D., Throl, U. and Raubach, H., *Acta Polymerica* **36**, 310 (1985).

[2] Friedrich, J. F., Loeschcke, I. and Gähde, J., *Acta Polymerica* **37**, 687 (1986).

[3] Gähde, J., Friedrich, J. F., Fischer, Th., Unger, W. E. S., Lippitz, A. and Falkenhagen, J., *Progr. Colloid and Polymer Science* **101**, 194 (1996).

[4] Lippitz, A., Koprinarov, I., Friedrich, J. F., Unger, W. E. S., Weiss, K. and Wöll, Ch., *Polymer* **37**, 3157 (1996).

[5] Koprinarov, I., Lippitz, A., Friedrich, J. F., Unger, W. E. S. and Wöll, Ch., *Polymer* **37**, 2005 (1997).

[6] Stöhr, J., *NEXAFS Spectroscopy*, Springer Series in Surface Science, Vol. 25 (Springer Verlag, Berlin 1992).

[7] Unger, W. E. S., Lippitz, A., Friedrich, J. F., Koprinarov, I., Weiss, K. and Wöll, Ch., *Metallized Plastics V*, Mittal, K. L. Ed. (VSP, Utrecht, The Netherlands 1998), p. 147.

[8] Dietz, E., Braun, W., Bradshaw, R. and Johnson, R. L., *Nucl. Instrum. Methods Phys. Res.* **A239**, 359 (1985).

[9] Jung, D. R. and Czanderna, A. W., "Interactions and Reactions at Metal/Self-assembled Organic Monolayer Interfaces", In: van Ooij, W. J. and Anderson, H. R. Jr., Eds., *Mittal Festschrift on Adhesion Science and Technology* (VSP, Utrecht, The Netherlands, 1998), pp. 717-746.

[10] Czanderna, A. W., King, D. E. and Spaulding, D., *J. Vac. Sci. Technol.* **A9**(5), 2607 (1991).

[11] King, D. E., Czanderna, A. W. and Spaulding, D., *J. Vac. Sci. Technol.* **A11**(1), 180 (1993).

[12] Gerenser, L. J., *J. Vac. Sci. Technol.* **5**, 2897 (1988).

[13] Chakraborty, A. K., Davis, H. T. and Tirell, M. J. J., *J. Polym. Sci., Part A: Polym. Chem.* **28**, 3185 (1990).

[14] Nowak, S., Collaud, M., Dietler, G., Gröning, P. and Schlapbach, L., *J. Vac. Sci. Technol.* **All**(3), 481 (1993).

[15] Akhter, S., Zhou, X.-L. and White, J. M., *Appl. Surf. Sci.* **37**, 201 (1989).

[16] Le, Quoc Toan, Chtaib, M., Pireaux, J. J. and Caudano, R. In: *Polymer-Solid Interfaces* Pireaux, J. J., Bertrand, P. and Bredas, J. L. Eds. (IOP Publishing, London, 1992).

[17] De Puydt, Y., Bertrand, P. and Lutgen, P., *Surf. Interf. Anal.* **12**, 486 (1988).

[18] Bou, M., Martin, J. M., Le Mogne, Th. and Vovelle, L., *Appl., Surf. Sci.* **47**, 149 (1991).

[19] Polzonetti, G., Russo, M. V., Furlani, A. and Infante, G., *Chem. Phys. Lett.* **214**(3–4), 333 (1993).

[20] Connor, J. A., Derrick, L. M. R. and Hillier, I. H., *J. Chem. Soc. Faraday Trans. II.* **70**, 941 (1974).

[21] Pignataro, S., Foffani, A. and Distefano, G., *Chem. Phys. Letters* **20**, 350 (1973).

[22] Albert, M. R. and Yates, J. T., *The Surface Scientist's Guide to Organometallic Chemistry* (American Chemical Society, Washington D.C., 1987).

[23] Mutterties, E. L., Bleeke, J. R., Wucherer, E. J. and Albricht, T. A., *Chem. Rev.* **82**, 499 (1982).

[24] Burdett, J. K. and Canadell, E., *Organometallics* **4**(5), 805 (1985).

[25] Kovac, C. A., Jordan-Sweet, J. L., Goldberg, M. J., Clabes, J. G., Viehbeck, A. and Pollack, R. A., *IBM J. Res. Develop.* **32**, 603 (1988).

[26] Mittal, K. L. and Lee, K.-W. Eds., *Polymer Surfaces and Interfaces: Characterisation, Modification and Application* (VSP, Utrecht, The Netherlands, 1997).

[27] Jordan, J. L., Sanda, P. N., Morar, J. F., Kovac, C. A., Himpsel, F. J. and Pollack, R. A., *J. Vac. Sci. Technol.* **A4**(3), 1046 (1986).

[28] Jordan, J. L., Kovac, C. A., Morar, J. F. and Pollack, R. A., *Phys. Rev.* **B36**, 1369 (1987).

[29] Manske, R. H., *Org. Syntheses, Coll. Vol. II.* 154 (1943).

[30] Briggs, D. and Seah, M. P., *Practical Surface Analysis* **1** (Wiley, Chichester, 1994).

[31] *Handbook of X-ray Photoelectron Spectroscopy*, Physical Electronics Inc., 1995.

[32] Unger, W. E. S., Lippitz, A. and Friedrich, J. F., *Materialprüfung* **37**, 6 (1995).

[33] Beamson, G. and Briggs, D., *High Resolution XPS of Organic Polymers* (Wiley and Sons, Chichester, 1992).

[34] Scofield, J. H., *J. Electron. Spectrosc. Relat. Phenom.* **8**, 129 (1976).

[35] Bernstorff, S., Braun, W., Mast, M., Peatman, W. and Schroeder, T., *Rev. Sci. Instrum.* **60**(7), 2097 (1989).

[36] Koprinarov, I., *Ph.D Thesis*, University of Potsdam (Germany), Potsdam, 1999, in press.

[37] Braun, W. and Koch, E.-E., *Nucl. Instrum. Methods Phys. Res.* **A261**, 115 (1987).

[38] Batson, P. E., *Phys. Rev.* **B48**, 2608 (1993).

[39] "Standard Terminology Relating to Surface Analysis", ASTM E 673-91c, *Annual Book of ASTM Standards* Vol. 03.06 (ASTM, Philadelphia, 1993).

[40] Seah, M. P. and Dench, W. A., *Surf. Interface Anal.* **1**, 2 (1979).

[41] Silvain, J. F., Ehrhardt, J. J. and Lutgen, P., *J. Adhesion Sci. Technol.* **5**, 501 (1991).

[42] Friedrich, J. F. In: *Polymer-Solid Interfaces*, Pireaux, J. J., Bertrand, P. and Bredas, J. L., Eds. (IOP Publishing, London, 1992).

[43] Sack, S., Wagner, H. and Steger, E. *Acta Polymerica* **36**, 305 (1985).

[44] Robert, T., *Chem. Physics* **8**, 123 (1975).

[45] Pireaux, J. J., *Synthetic Metals* **67**, 39 (1994).

[46] Unger, W. E. S., Lippitz, A., Friedrich, J. F., Koprinarov, I., Weiss, K. and Wöll, Ch. In: *Metallized Plastics V*, Mittal K. L. Ed. (VSP, Utrecht, The Netherlands, 1998), p. 147.

[47] Liu, A. C. and Friend, C. M., *J. Chem. Phys.* **89**, 4396 (1988).

[48] Friend, C. M. and Roberts, J. T., *Acc. Chem. Res.* **21**, 394 (1988).

[49] Friedrich, J. F., Unger, W. E. S., Lippitz, A., Geng, Sh., Koprinarov, I., Kühn, G. and Weidner, St., *Surface Coat. Technol.* **98**, 1132 (1998).

[50] Unger, W. E. S., Lippitz, A., Gross, Th., Friedrich, J. F., Wöll, Ch. and Nick, L., *Langmuir* **15/4**, 1161 (1999).

[51] Friedrich, J. F., Unger, W. E. S., Lippitz, A., Koprinarov, I., Weidner, St., Kühn, G. and Vogel, L. In: *Metallized Plastics V*, Mittal, K. L. Ed. (VSP, Utrecht, The Netherlands, 1998), p. 271.